

# Stability and Characteristics of Large CZT Coplanar Electrode Detectors

José M. Pérez, Zhong He, *Senior Member, IEEE*, and David K. Wehe, *Senior Member, IEEE*

**Abstract**—The single polarity charge sensing method based on coplanar grid electrodes has demonstrated promising results on CZT detectors having volumes of  $\sim 1 \text{ cm}^3$ . This paper presents the performance of two coplanar grid CZT detectors having dimensions of  $1.5 \times 1.5 \times 1.0 \text{ cm}^2$ , among the largest CZT spectrometers that have been reported. Energy resolutions of 2.3% and 2.0% full-width half-maximum were obtained on the two detectors at 662 keV using simple analog techniques. Further improvement is achievable with depth sensing and digital pulse processing techniques. Other detector characteristics, critical to practical application of these devices, are reported here. This includes the stability of detector response over a period of several months and the variation of detector performance in environments having high gamma radiation fluxes and a range of counting rates.

**Index Terms**—Gamma-ray spectroscopy detectors, radiation effects, semiconductor radiation detectors, stability.

## I. INTRODUCTION

**R**ADIATION detectors based on room temperature semiconductors with high atomic numbers have been under development for the past two decades.  $\text{HgI}_2$ , CdTe and CdZnTe detectors have been successfully utilized in various applications.

The widespread use of this type of detector has been hindered by charge trapping properties. Typical mobility-lifetime products for holes in these materials are one order of magnitude lower than that for electrons. As this limitation is inherent in these materials, methods to overcome hole trapping have been explored. The single polarity charge sensing method, based on the coplanar grid electrodes proposed by Luke [1], yielded a dramatic improvement in energy resolution. The introduction of depth sensing techniques [2], [3] extended the capability of this method and added a powerful tool for characterizing and enhancing detector performance.

Although improvements can be expected from more efficient detector designs and material advances, the energy resolution of current generation coplanar electrode CdZnTe detectors already allows their practical application in the range of 60 to 1500 keV. But other properties are also required in practical applications, the most important of which are 1) detection efficiency, 2) implementation complexity, and 3) reliability and stability. This paper describes work on two large coplanar grid CdZnTe detec-

tors to more fully characterize their performance for practical applications.

- 1) Good intrinsic efficiency is inherent to CdZnTe detectors due to their high atomic number. Moreover, a large volume is also required for assuring a high absolute efficiency. Each of the two detectors employed in this paper has a volume of  $2.25 \text{ cm}^3$ , among the largest CZT spectrometers that have been reported.
- 2) When considering complexity, the use of coplanar grid detectors requires only simple electronic enhancements compared to a conventional planar detector: a dual preamplifier unit, coupled to a subtraction circuit [2], replaces the single preamplifier unit used in standard planar detectors.
- 3) Two experiments were performed to study reliability and stability, characteristics critical to the practical application of these devices. This study examined the detector stability over a period of several months, along with the variation of performance when operating at different counting rates in environments with high gamma fluxes. Changes in the basic spectral properties observed during the experiment are reported herein.

## II. EXPERIMENTAL SETUP

Two coplanar electrode CdZnTe detectors having dimensions of  $1.5 \times 1.5 \times 1.0 \text{ cm}^3$  were used in this work. The detectors (I9-01 and I9-04) were manufactured by eV Products<sup>1</sup> using the Generation II [4] coplanar electrode design. Two preamplifier units were constructed, each using three A250 AMPTEK preamplifiers and a subtraction circuit. Both coplanar electrodes and the cathode were ac-coupled to each corresponding preamplifier. Output signals from the anode preamplifiers were subtracted in order to implement Luke's coplanar anode method [1]. The relative gain of the two anode signals was adjusted using a potentiometer. The cathode signal was only used for the digital studies described later.

One of the preamplifier modules was connected to detector I9-01 and used for spectroscopic testing and digital studies. The second module, connected to the I9-04 detector, was designed for the accurate stability tests. In this second module, more precise electronic components were used in the subtraction circuit, which permitted fine adjustments and a constant relative gain of the anodes.

All the spectra presented in this paper were acquired using a 672 ORTEC Gaussian amplifier<sup>2</sup> with  $1 \mu\text{s}$  shaping time. The

Manuscript received October 23, 2000; revised January 23, 2001 and March 13, 2001. This work was supported in part by the Spanish Ministry of Education under Grant PR 1999-0177 0076243636 and in part by the U.S. Department of Energy under Grant DE-FG08-98NV 13357.

J. M. Pérez is with CIEMAT, Madrid E-28040, Spain (e-mail: jm.perez@ciemat.es).

Z. He and D. K. Wehe are with the Department of Nuclear Engineering and Radiological Sciences, The University of Michigan, Ann Arbor, MI 48109 USA.

Publisher Item Identifier S 0018-9499(01)04774-8.

<sup>1</sup>eV Products, Saxonburg, PA.

<sup>2</sup>Perkin-Elmer Instruments, Oak Ridge, TN.

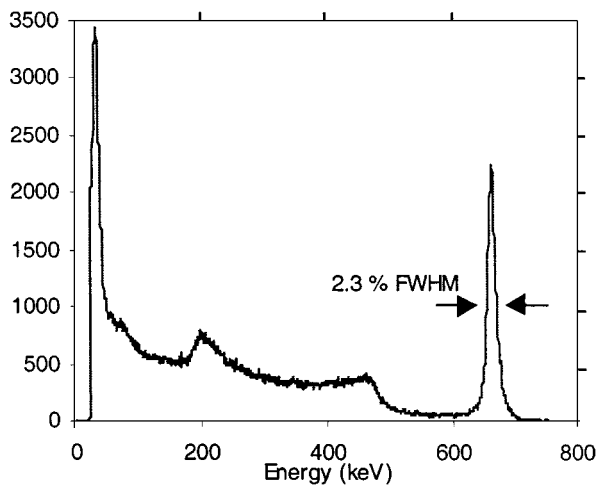


Fig. 1. Representative  $^{137}\text{Cs}$  spectrum acquired with detector I9-04.

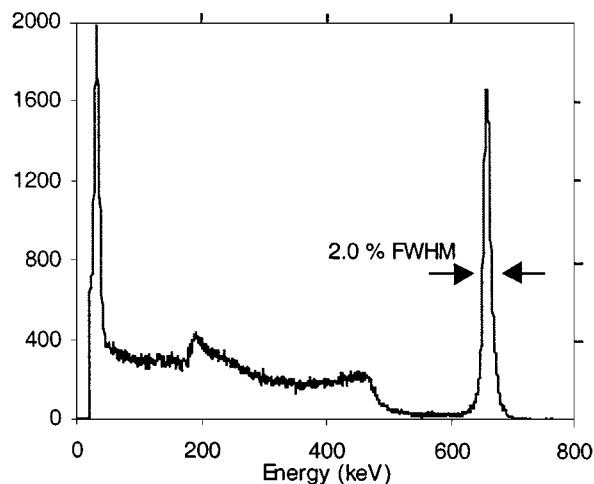


Fig. 2. Representative  $^{137}\text{Cs}$  spectrum acquired with detector I9-01.

noncollecting anode and cathode biases were set to  $-80\text{ V}$  and  $-1700\text{ V}$ , respectively, while the collecting anode was set at  $0\text{ V}$ . Precise mechanical supports for the detector and sources were constructed to permit periodic calibration tests by changing the source while ensuring a fixed source–detector geometry.

### III. SPECTROSCOPIC PERFORMANCE

#### A. Resolution

The two detectors were first tested as spectrometers. The relative anode gain was chosen to optimize spectroscopic resolution at higher gamma energies (662 to 1333 keV). Representative results are shown in Figs. 1 and 2. Detectors I9-04 and I9-01 exhibited energy resolutions of 2.3% and 2.0% for the 662 keV  $^{137}\text{Cs}$  peak, respectively.

#### B. Energy Linearity

Energy linearity was excellent in both detectors. Results only for the I9-01 detector are presented. A spectrum using three radioactive sources simultaneously— $^{133}\text{Ba}$ ,  $^{137}\text{Cs}$ , and  $^{60}\text{Co}$ —was acquired and is displayed in Fig. 3. The spectrum was acquired with a TRUMP-PCI-8k multichannel card, and

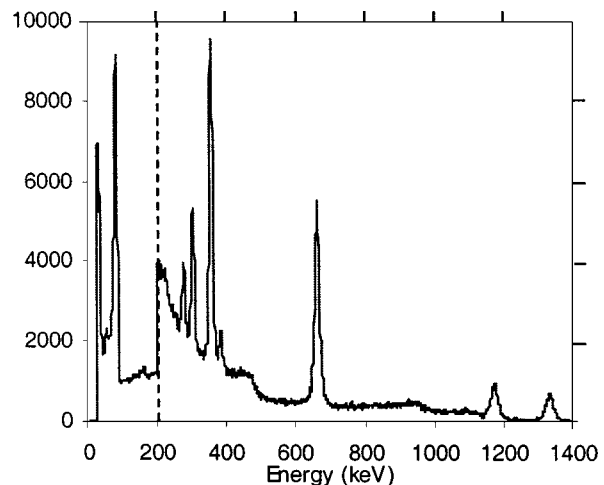


Fig. 3. Spectrum acquired irradiating detector I9-01 with  $^{137}\text{Cs}$ ,  $^{60}\text{Co}$ , and  $^{133}\text{Ba}$  sources simultaneously. The spectrum is shown magnified 3.5 times above 200 keV.

TABLE I  
ENERGY CALIBRATION

Energy Line	Centroid Position
80.9	79.29
302.8	303.52
356.0	356.33
1173.2	1173.66
1332.5	1333.15

Maestro-32 software [6] was used for the peak identification and centroid search.

The energy calibration for this spectrum used only the  $^{137}\text{Cs}$  photopeak. The centroid obtained for this peak was assigned to 661.66 keV. Table I shows the corresponding energy values for the centroids of the other evident peaks in Fig. 3. The radiation energies reported in [5] for the isotopes were used in this table.

#### C. Major Differences in Spectra

Detectors I9-01 and I9-04 show very similar but not identical spectroscopic performances. Fig. 1 shows more counts near the X-ray peak than Fig. 2 does. Background measurements revealed that this difference is not due to background effects.

A digital study of pulse shapes indicated the likely cause of this difference. Pulses at the anodes and cathode preamplifier outputs were digitized and processed in a PC. The acquisition system was implemented by connecting a digital oscilloscope (Infinium 54 845A)<sup>3</sup> to a computer using an IEEE-488 GPIB interface. Algorithms for measuring the amplitude of each individual pulse were written in C++, together with routines that implement digital Gaussian shaping filters and digital versions of the spectroscopic method used in this paper [1] and the depth sensing technique used in [2] and [3]. The location of the pulse’s critical points and the digital Gaussian shaping were implemented using the wavelet algorithms presented in [6] and [7].

Typical pulses from the anodes and cathode outputs are shown in Fig. 4. These particular pulses correspond to a photon interacting near the cathode side of the detector. These shapes

<sup>3</sup>Agilent Technologies, Englewood, CO.

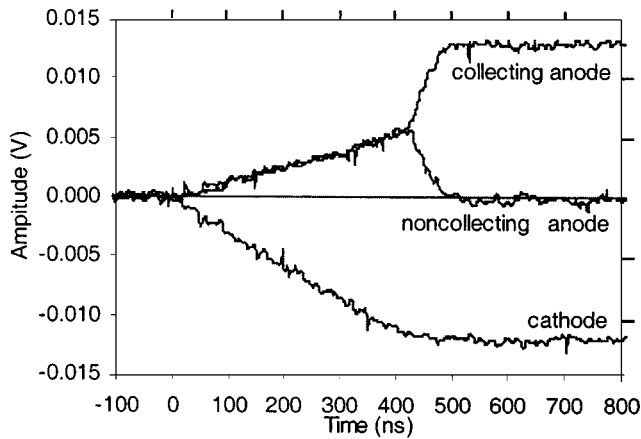


Fig. 4. Charge pulses with expected shapes generated at the preamplifier outputs by a photon interacting near the cathode.

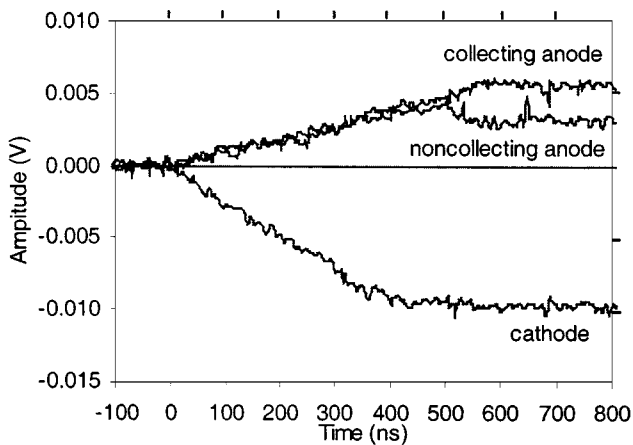


Fig. 5. Charge pulses with unexpected shapes.

are consistent with charge pulses reported in previous work (see [1] and [8]).

However, events in which the generated pulses do not follow the expected profiles were also experimentally observed in detector I9-04. In some cases, pulses from the noncollecting anode end with a significant positive net contribution, although a zero or negative net amplitude is expected. Fig. 5 shows one such example. Spectra using pulses only with this unexpected shape have been collected. These pulses, generated by photons interacting only near the cathode, revealed that the positive contribution in the unexpected noncollecting-anode pulses extended from zero up to almost the full expected collecting-anode pulse height. Different spectra were acquired by choosing only those pulses with selected levels of this unexpected behavior. A qualitative correlation exists between the spectroscopic response for those events in which the noncollecting-anode pulse presents a large positive value and the enhanced low pulse height population displayed in Fig. 1 relative to Fig. 2. This pulse height distribution shift became wider and spread to higher energies as the noncollecting-anode residual amplitude was closer to zero.

#### IV. DETECTOR STABILITY

Detector I9-04 was studied for four months to check possible drifts in the main spectroscopic properties. During the exper-

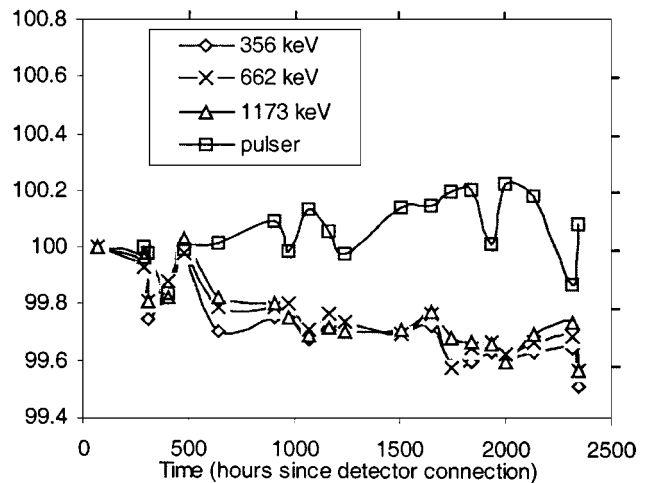


Fig. 6. Evolution of the photopeak position during the experiment.

iment, all parameters in the electronic chain remained fixed. Temperature was maintained at  $22.5 \pm 1.0$  °C. The detector box was shielded with a 5-cm-thick layer of lead around all surfaces, except the upper side, where 10 cm was used. This shielding permitted a low background count rate even at medium and high energies. A precision pulser (Ortec 419) was used to test for possible detector instabilities from electronic drift. Periodic checks were performed with three radioactive sources ( $^{133}\text{Ba}$ ,  $^{137}\text{Cs}$ , and  $^{60}\text{Co}$ ). Data obtained from the 356-, 662-, and 1173-keV lines were used for checking the detector performance. The results are presented below.

##### A. Photopeak Position

The shift of the 356-, 662-, and 1173-keV photopeak position during the experiment is presented in Fig. 6, together with the values for the pulser peak. Peak centroid shifts smaller than 0.5% occurred during the 2500 h after detector bias. Note that the drift is similar for all three energies, but the values obtained for the pulser peak centroid remained closer to the initial value.

##### B. Energy Resolution

Larger variations were observed in energy resolution. Fig. 7 presents results relative to the values measured in the initial stable spectrum. The counting rates for the 356- and 662-keV photopeaks were 650 and 430 cps, respectively. For the 1173-keV and pulser peaks, the counting rate is only 60 cps. The lower counting rates contributed to larger fluctuations in 1173-keV and pulser peaks during the short acquisition times used (100 s in all the spectra in this work). Peak width was measured directly on the spectrum raw data, without applying any peak fitting algorithm. This contributes to fluctuations in the resolution's being much larger than obtainable using peak fitting (see [9]). Fig. 7 shows that the fluctuations in energy resolution are largest at higher energies.

To clarify the relative importance of the fluctuations shown in Fig. 7, Fig. 8 compares the two  $^{60}\text{Co}$  spectra corresponding to the two extreme cases on the 1173-keV curve in Fig. 7, i.e., those points marked in black. It can be seen that the differences between these two spectra are relatively insignificant. The 1173-keV photopeak areas differ by less than 2%, while the dif-

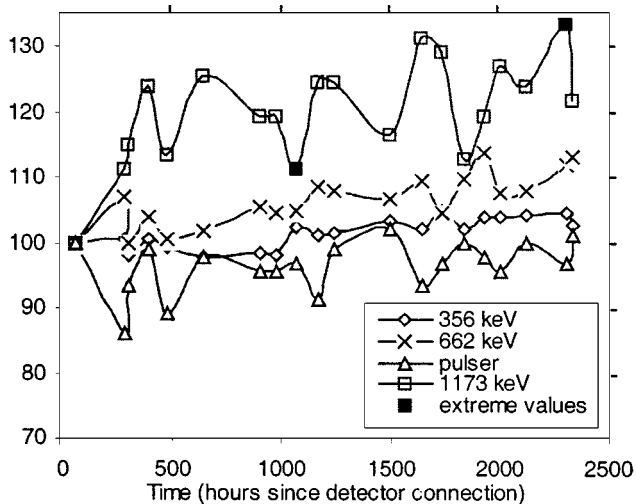


Fig. 7. Evolution of the detector resolution relative to the initial value. Extreme values in the 1173-keV data fluctuations are highlighted in black.

ference in the centroid positions is less than 0.1%. This example shows that the resolution variations in Fig. 7 are not associated with dramatic changes in the detector spectroscopic performance. However, the data in Fig. 7 show that the energy resolution did degrade over time. This tendency was apparent at higher energies and negligible for the 356-keV and pulser peaks. This last result confirms that the electronic noise contribution remained approximately constant during the experiment. Thus, factors related to the detector’s electrical properties caused the resolution shift.

### C. Photopeak Efficiency

Changes in the counting rate for three photopeaks are presented in Fig. 9. Note that the source activity decayed during the experiment by 1.6%, 0.6%, and 3.2% for the  $^{133}\text{Ba}$ ,  $^{137}\text{Cs}$ , and  $^{60}\text{Co}$  sources, respectively. The fluctuations shown in Fig. 9 are partially attributable to statistics and to uncertainties intrinsic to the determination of the photopeak area. The peak identification algorithms in the Aptec PCMCA/Super Application Software<sup>4</sup> were used with standard search parameters. Some difficulties were encountered during the area search for the 1173 peak, due to its particular position in the  $^{60}\text{Co}$  spectrum. Its net area calculation can be distorted by interference with the 1333-keV peak and Compton edge.

The detector displayed an increase in efficiency during the initial period of operation, but the efficiency seemed to decrease after longer times. In any case, the large fluctuations in the data, mainly in the 1173-keV data, preclude any definitive conclusion.

### D. Background

The I9-04 detector was tested for stability by performing background measurements during the experiment. The initial count rate, in the absence of radioactive sources, was 0.27 cps over the 60–2000 keV range. Repeated measurements performed during the experiment (2500 h) under the same

<sup>4</sup>Aptek—NCR, Warrington, PA.

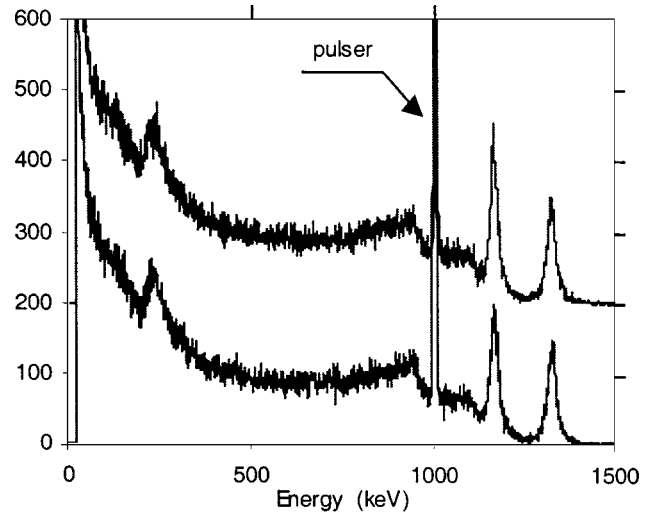


Fig. 8.  $^{60}\text{Co}$  spectra corresponding to the data marked in black on the 1173-keV curve in Fig. 7.

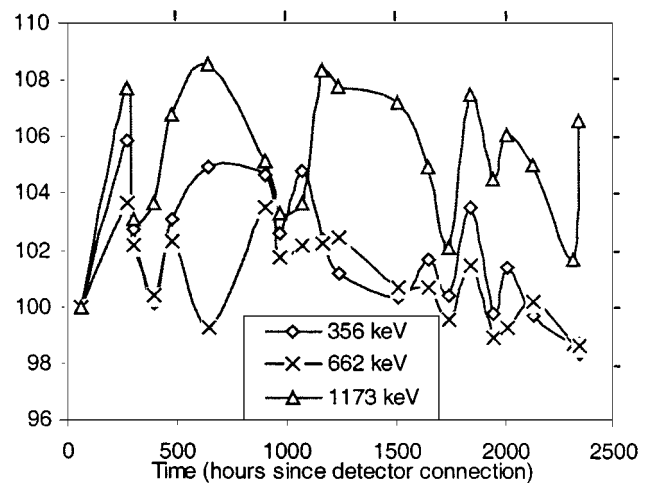


Fig. 9. Evolution of the peak counting rates.

conditions showed fluctuations smaller than 5% relative to this initial value.

Occasionally, the detector showed fluctuations that seriously distorted the background spectrum. Pulses not due to charge produced by radiation were observed, contributing to the spectrum by generating counts at different energies. The frequency of these fluctuations was variable, roughly every other week. The influence on the spectrum was variable. Fig. 10 presents the background spectrum acquired during 20 s during one of these unstable states. It is compared in the same figure with results from a long background measurement (21 600 s) acquired under normal conditions. These fluctuations disappeared naturally after some time. We have not isolated the cause of these anomalies.

## V. PERFORMANCE UNDER MEDIUM AND HIGH RADIATION FLUXES

### A. Spectroscopy at High Counting Rates

The detector capability as a spectrometer in high radiation fields was also tested. A  $^{137}\text{Cs}$ , 164 mCi source was used for

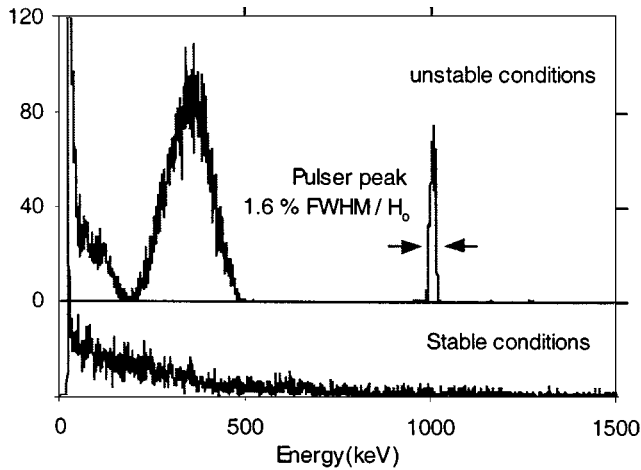


Fig. 10. Comparison of a short background measurement obtained in unstable conditions versus the general detector response.

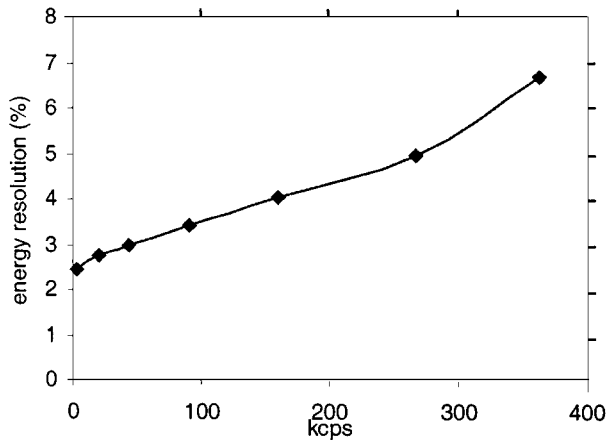


Fig. 11. Detector energy resolution for 662 keV versus different counting rates.

this purpose. Figs. 11 and 12 present the changes observed in the 662-keV photopeak resolution and position in the spectra acquired at counting rates up to 363.5 kcps in the 60–2000 keV range. Spectra acquired at different counting rates are compared in Fig. 13. Spectra in this figure were acquired using the pile-up rejector output in the Ortec 672 spectroscopy amplifier [5]. Shifts observed in Fig. 13 at different counting rates are not related to changes in detector performance but are due to electronics effects. The irradiation did not affect the detectors' performance—no changes were observed in the detector gain, resolution, efficiency, or background measurements after these irradiations.

### B. Effects of Irradiation with High Fluxes

To check possible changes caused by long exposure to high radiation fluxes, the detector was irradiated with a hot  $^{60}\text{Co}$  source. The integrated dose that the detector absorbed in the complete test was  $\sim 10\,000$  rad. This dose is far below the expected value needed to damage the detector, but is a more realistic value for the dose that a detector might absorb during its working life in many practical applications.

The irradiation was performed in 11 sessions, at a dose rate of 5840 rad/h. The detector was maintained biased during the irra-

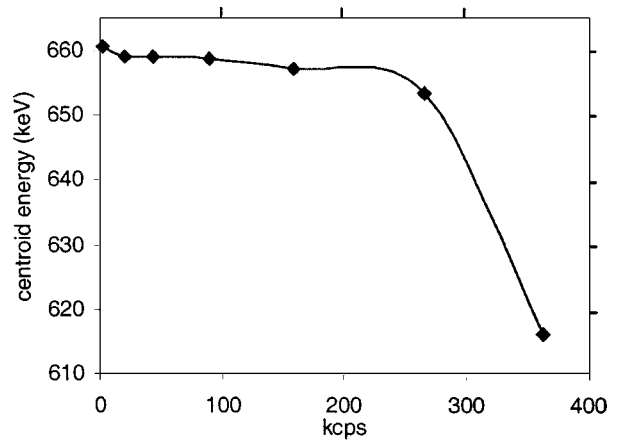


Fig. 12. The 662-keV photopeak position at different counting rates.

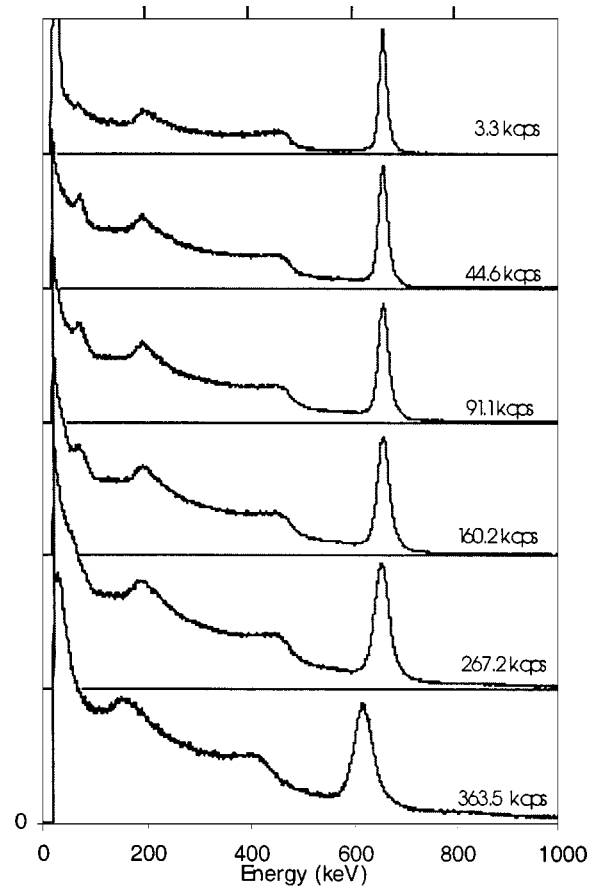


Fig. 13.  $^{137}\text{Cs}$  spectra acquired at different counting rates.

diation, although the preamplifiers were disconnected. Spectra were repeatedly acquired during 30-s intervals, using a calibrated  $^{137}\text{Cs}$  source, from the end of each irradiation until 30 min. After this time, the next irradiation was started.

Fig. 14 shows the observed drifts in the peak centroids for the 662-keV line and the pulser peak. The detector system reveals a consistent centroid shift to lower channels for both peaks. After this test, the detector was removed and the complete electronic chain was irradiated in two identical sessions. As expected, there was no evidence of change. This demonstrates that the reported drifts are only due to changes in the detector.

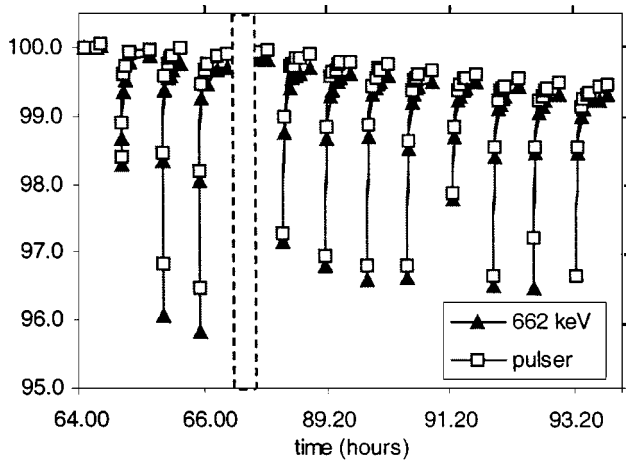


Fig. 14. Evolution of the 662-keV and pulser peak positions during the irradiation test. The discontinuity represented with a blank vertical bar corresponds to an overnight period between the hours 66.3 and 88.1 from the experiment's start.

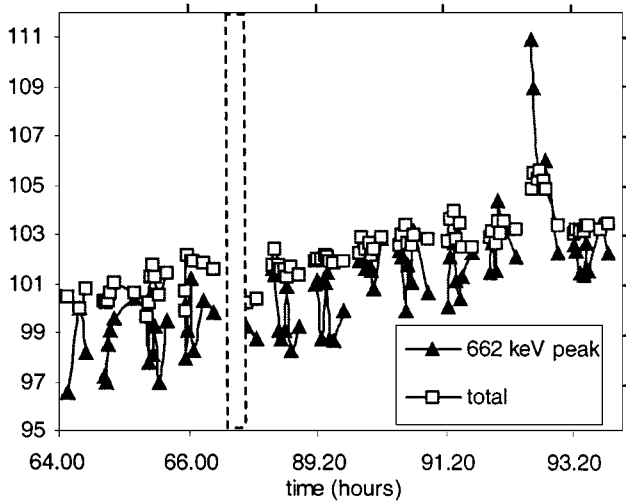


Fig. 15. Evolution of the total (60–2000 keV) and 662-keV peak counting rate during the irradiation test. The discontinuity represented with a blank vertical bar corresponds to an overnight period between the hours 66.3 and 88.1 from the experiment's start.

A continuous increase in both the photopeak and the total count rate was observed during the irradiation. Fig. 15 shows these changes.

## VI. CONCLUSION

The detectors presented in this paper showed excellent resolution, among the best values reported for a CZT detector with similar dimensions. Detector I9-04 was sufficiently reliable for practical uses. But important instabilities during the long background measurements were observed. This behavior is not a major limitation for many applications, since the detector is not permanently affected, but it may be problematic if long acquisition times and low count rates are involved.

## ACKNOWLEDGMENT

The authors wish to acknowledge the support of the University of Michigan Phoenix Project, particularly H. Downey, R. Blackburn, and C. Weger for their invaluable assistance during the irradiations.

## REFERENCES

- [1] P. N. Luke, "Unipolar charge sensing with coplanar electrodes: Application to semiconductor devices," *IEEE Trans. Nucl. Sci.*, vol. 42, pp. 207–213, Aug. 1995.
- [2] Z. He, G. K. Knoll, D. K. Wehe, R. Rojeski, C. H. Mastrangelo, M. Hamming, C. Barret, and A. Uritani, "1-D position sensitive single carrier semiconductor detectors," *Nucl. Instrum. Meth. A*, vol. 380, pp. 228–231, 1996.
- [3] Z. He, G. K. Knoll, D. K. Wehe, and J. Miyamoto, "Position-sensitive single carrier CdZnTe detectors," *Nucl. Instrum. Meth. A*, vol. 388, pp. 180–185, 1997.
- [4] Z. He, G. K. Knoll, D. K. Wehe, and Y. F. Du, "Coplanar grid pattern and their effect on energy resolution of CdZnTe detectors," *Nucl. Instrum. Meth. A*, vol. 411, pp. 107–113, 1998.
- [5] National Nuclear Data Center, Brookhaven National Laboratory, Upton, NY 11973–500, USA.
- [6] G. García-Belmonte, J. M. Pérez, J. Marín, and J. L. F. Marrón, "Gaussian filter bank design using the discrete wavelet transform for improving CZT-gamma ray detector spectroscopy response," *Nucl. Instrum. Meth. A*, vol. 396, pp. 272–276, 1997.
- [7] J. M. Pérez and G. García-Belmonte, "Pulse filtering and correction for CZT detectors using simple digital algorithms based on the wavelet transform," in *Proc. MRS*, vol. 487, 1998, pp. 187–192.
- [8] P. N. Luke, "Single-polarity charge sensing in ionizing detectors using coplanar electrodes," *Appl. Phys. Lett.*, vol. 65, no. 22, pp. 2884–2886, Nov. 1994.
- [9] G. K. Knoll, *Radiation Measurement and Detection*, 3 ed. New York: Wiley, 2000, p. 709.